

JOURNAL OF ADVANCED APPLIED SCIENCES

e-ISSN: 2979-9759



RESEARCH ARTICLE

The Structural Examination of Fe/(Cu/Nb)/MgB₂ Multifilament Wires During Cold Forming Process

Doğan Avcı^{1™} • Hakan Yetiş² • Fırat Karaboğa³ • İbrahim Belenli² •

ARTICLE INFO

Article History

Received: 06.12.2023 Accepted: 20.02.2024 First Published: 06.05.2024

Keywords

В

Cold forming

Mg

MgB2 wire

Superconductivity

Transport measurements



ABSTRACT

In this study, we have successfully produced a Fe-sheathed 6+1 multifilament wire using Cu/Nb/MgB $_2$ monocore wires. The mono filament wire was prepared using Mg+2B powder mixture by powder-in-tube method without any intermediate heat treatment. The powder mixture of the amorphous nano boron (PVZ Nano Boron, purity of 98.5%, particle sizes < 250 nm) and high purity Mg powder (PVZ Mg, purity of 99%, particle size 74 μ m) were used. The multifilament wire was produced using groove rolling and cold drawing machines. The geometrical form of the filaments was examined using wire pieces taken from the wire at different steps throughout the production process. Finally, the multifilament wires produced in two different diameters of 1.02 mm and 0.82 mm were investigated in terms of filament uniformity, crack formation, surface roughness, and electrical transport properties. The structural examination was done on Nb filaments after the Fe and Cu sheaths were etched using HCl and HNO $_3$ solution. The I – V measurements of the multifilament wires heat treated at 650 °C for 15, 30, 45, 60, and 240 minutes, and 700 °C for 60 minutes were carried out for the applied current up to 1 A at 25 K under various external magnetic field.

Please cite this paper as follows:

Avcı, D., Yetiş, H., Karaboğa, F., & Belenli, İ. (2024). The structural examination of Fe/(Cu/Nb)/MgB₂ multifilament wires during cold forming process. *Journal of Advanced Applied Sciences*, *3*(1), 15-22. https://doi.org/10.61326/jaasci.v3i1.127

1. Introduction

Following the discovery that MgB₂ is a superconductor, various forms of MgB₂ have been fabricated, including bulk structures, thin films, tapes, and wires (Feng et al., 2003; Nakane et al., 2005; Xi, 2009; Koblischka et al., 2014). Among these, MgB₂ in wire form stands out as a particularly promising superconducting material for magnet applications due to its utilization of cost-effective raw materials and its straightforward production processes (Vinod et al., 2007; Yao et al., 2010; Patel et al., 2014). In the realm of technological

applications, the production of long multifilament wires is mandatory to reduce AC losses (Jiawen et al., 2019). Various manufacturing techniques, such as the powder-in-tube (PIT) process and continuous tube filling forming (CTFF) process, have been employed in the production of MgB₂ wire. The CTFF process allows the fabrication of long wires, but controlling the initial filling density is challenging (Suo et al., 2007; Tomsic et al., 2007). To advance the development of superconducting devices utilizing MgB₂ wire, there is a need for multifilament wire created from high-density monofilaments to enhance the

E-mail address: davci.0209@gmail.com



¹TÜBİTAK National Metrology Institute, Quantum Metrology Laboratory, Kocaeli/Türkiye

²Bolu Abant Izzet Baysal University, Faculty of Arts and Sciences, Department of Physics, Bolu/Türkiye

³Bolu Abant İzzet Baysal University, Mehmet Tanrıkulu Vocational School of Health Services, Bolu/Türkiye

[™] Correspondence

critical current density $(J_c(B))$. Investigating the structural properties of MgB2 filaments is crucial to advance the development of MgB₂ filaments. The deformations during the production process are highly effective on the electrical performance of MgB₂ wire (Goldacker et al., 2004a). Filament size, geometrical alignment, filament integrity, and sausage effects related to wire structure can be easily explored using the optical microscopy and scanning electron microscopy, but these methods are destructive. Masayoshi and Yuichi (2023) conducted a study involving an MgB2 wire with 18 filaments, utilizing X-ray computed tomography (CT) to observe deformations such as sausage effects and filament breakage points on the filament surfaces. X-ray CT is effective as a nondestructive method for detecting deformations, but it is not sufficient to definitely distinguish types of deformation, such as cracks or sausages.

In this study, we used an etching technique to understand the origin of deformations in the filaments. The 6 filament Fe/Cu/Nb/MgB $_2$ multifilament wire was produced using both cold drawing and rolling methods without any intermediate heat treatment. The iron (Fe) and copper (Cu) sheaths were selectively etched using a hydrochloric acid (HCl) and nitric acid (HNO $_3$) solution, to expose the niobium (Nb) filaments. We examined the deformities arising during the cold-forming process on Nb filaments for different wire diameters. The electrical performance of the multifilament superconducting wires was tested by R-T and I-V measurements.

2. Materials and Methods

The mono-filament MgB_2 wire used for making the multifilament wire was fabricated with Cu/Nb sheaths.

Amorphous nano-boron powder (98% purity, < 250 nm size) and magnesium powder (99% purity, 74-144 µm size) were mixed according to the stoichiometric ratio (Mg+2B) using ball milling for 3 hours (Agate ball ratio 1:4, 200 rpm). The prepared powder mixture was filled into Nb tube (outer/inner diameter: 8/5 mm), and the Nb tube was placed into a Cu tube (outer/inner diameter: 12/8.30 mm). The Cu/Nb/Mg+2B sample was drawn from 12 mm to 1.94 mm without any intermediate heat treatment. The six wire pieces were then cut from the monofilament wire and the pieces were placed into a Fe tube (outer/inner diameter: 8/6 mm) with a Cu rod having diameter of 1.94 mm. The Cu rod was used as a stabilizer at the center of the filaments. Finally, the multifilament wire was produced for two different diameters of 1.02 and 0.82 mm by using cold drawing and rolling machines without any intermediate heat treatment as represented in Figure 1. During the cold forming processes, some pieces with diameters of 3.62 mm, 2.71 mm, 2.32 mm, and 1.50 mm were cut from the multifilament wire for the surface examination of Nb filaments (see Figure 2). The electrical measurements were performed on the wires with diameters of 1.02 mm and 0.82 mm, which were heat treated at 650 °C for 15-30-45-60-240 min. and at 700 °C for 60 min. Resistivity $(\rho - T)$ measurements were carried out between 10 and 45 K by applying 500 mA of DC current. The current-voltage (I - V) measurements were performed at 25 K under external magnetic field by applying a maximum 1 A DC current. Structural analyses were performed on the cross-sectional surface of the wires and the longitudinal section of Nb filaments by using optical microscopy before heat treatments.

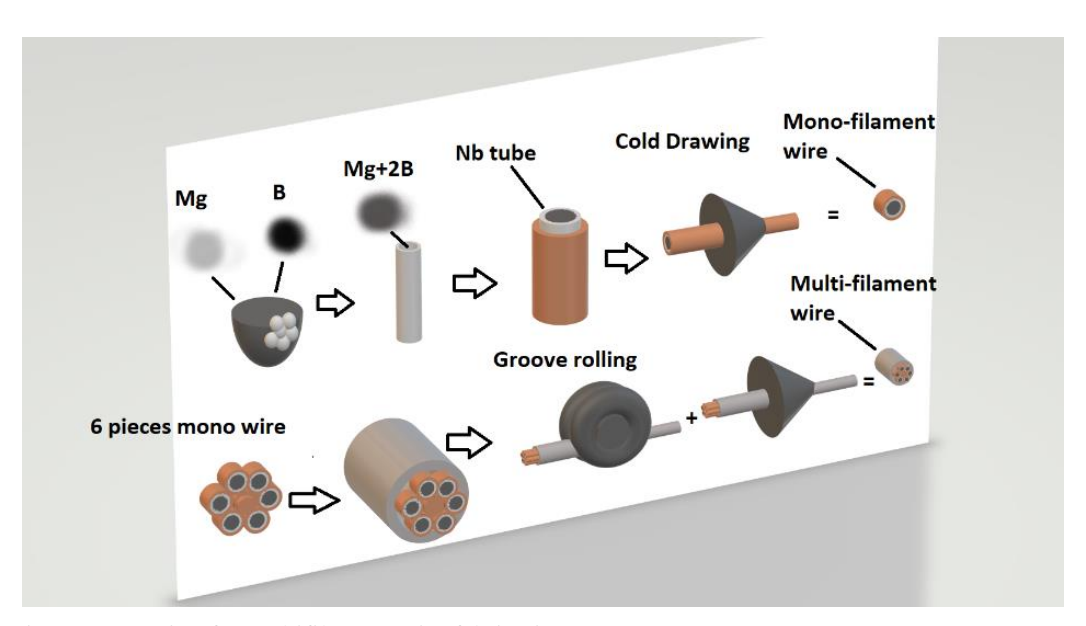


Figure 1. Schematic representation for multifilament wire fabrication.

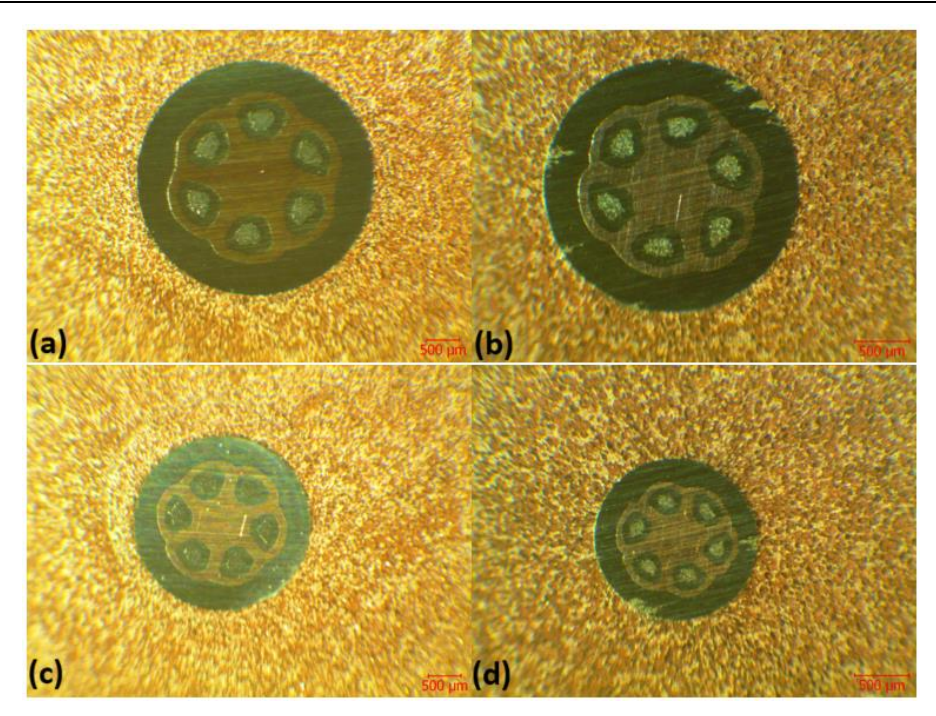


Figure 2. Surface images of wire pieces cut in different diameters during the cold forming process. The wire diameters are (a) 3.62 mm, (b) 2.71 mm, (c) 2.32 mm, and (d) 1.50 mm, respectively.

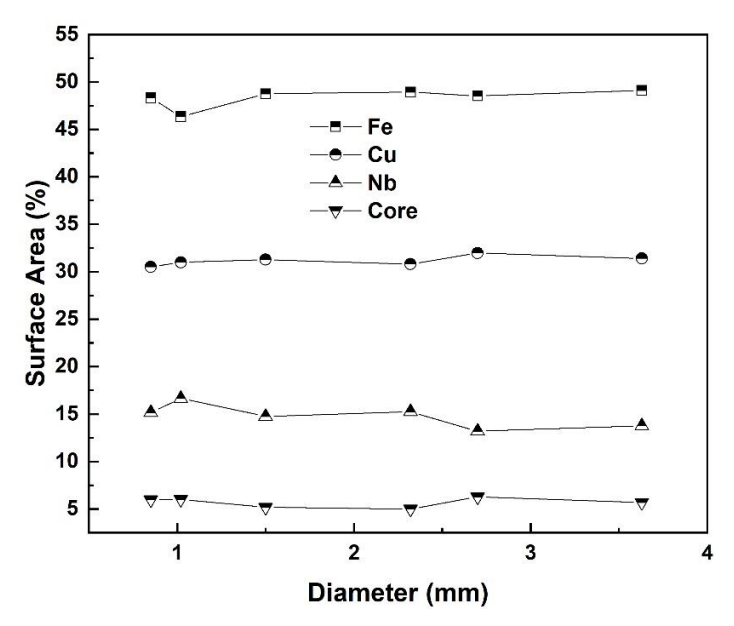


Figure 3. The percentage ratio of surface area of materials at different wire diameters.

The metallic cladding parts of the multifilament wires occupy 94% of the total cross-sectional area as shown in Figure 3. This also means that the superconducting MgB₂ content of the wire is only 6%. The fact that the cross-sectional areas of the core and metal components remain proportionally constant at different diameters is an indication that the extension/compression ratio is maintained.

3. Results and Discussion

Figures 4(a) and (b) illustrate the ρ – T curves of Fe/Cu/Nb/MgB₂ multifilament wires heat treated at different

annealing temperature and time. It is seen from Figures 4(a) and (b), all wires showed transition from normal to superconducting state in self-magnetic field. The zero resistivity is achieved at temperatures between 34 K and 35 K for all wires. The inset graphs in Figures 4(a) and (b) indicate the presence of a sharp superconducting transition for all wires. The superconducting transition width (ΔT) was determined to be below 1 K. The wires heat treated at 650 °C for 1h or less have slightly lower $T_{\rm c}$ values than wires heat-treated at 650 °C for 240 min. and 700 °C for 60 min. This difference in $T_{\rm c}$ became more pronounced in wires with a diameter of 0.82 mm. The steep linear increase in normal state resistivity with increasing

temperature and the low $\rho(40~{\rm K})$ value of 0.15 $\mu\Omega$.cm are result of the high metallic content of the wires.

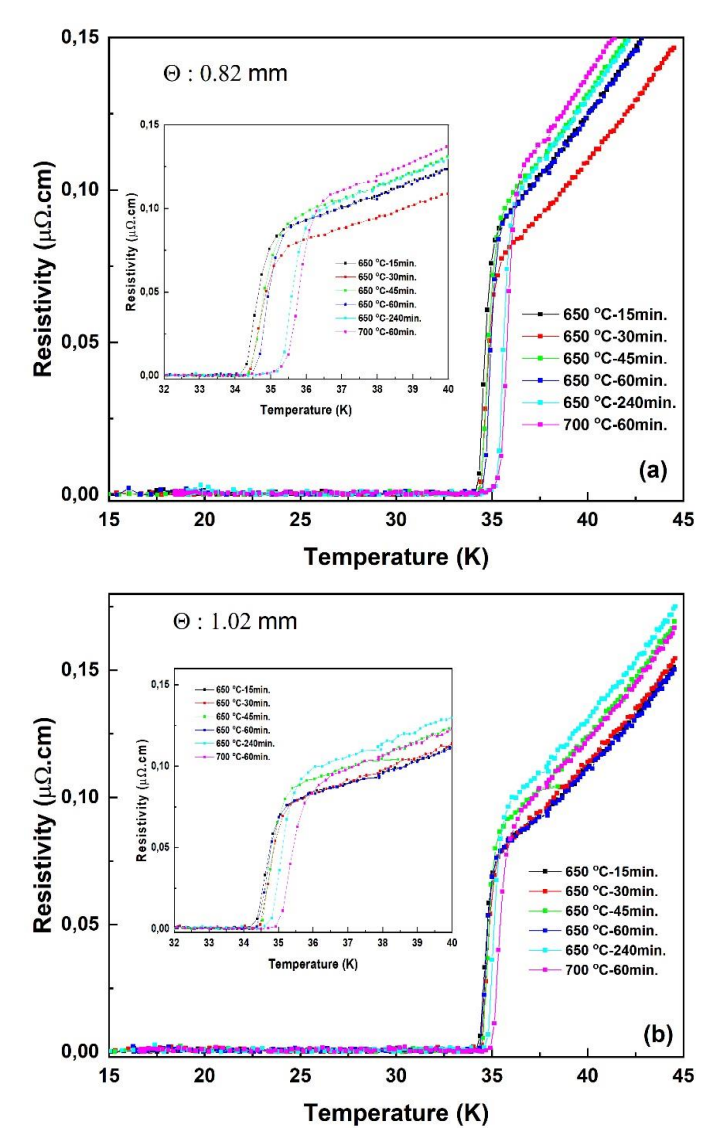


Figure 4. The resistivity vs. temperature curves of multifilament wires produced for two different diameters of (a) 0.82 and (b) 1.02 mm. The wires were heat treated under different conditions.

Figures 5(a) and (b) show the E-I curves obtained at 25 K under 3.75 T for the wires with diameters of 0.81 mm and 1.02 mm, respectively. Different sections of the multifilament wire were used for each E-I measurement. It is observed that there are some changes on the transport properties of Fe/Cu/Nb/MgB₂ multifilament wires annealed under different heat treatment conditions. It may be thought that the changes in I_c values may be caused by differences in heat treatment conditions, but this is not evident in the E-I measurements obtained with an applied current of 1 A. As seen in Figure 5(b), the I_c value of the wire annealed at 650 °C for 15 min. is the same as that of the wires annealed at 700 °C for 60 min. and 650 °C for 60 min. On the other hand, it is evident that the diameter of the wire directly influences its transport properties,

as decreasing wire diameter leads to an increase in core density. As seen in Figures 5(a) and (b), the I_c values of the wires under external magnetic field decreases when the wire diameter is reduced from 1.02 mm to 0.82 mm.

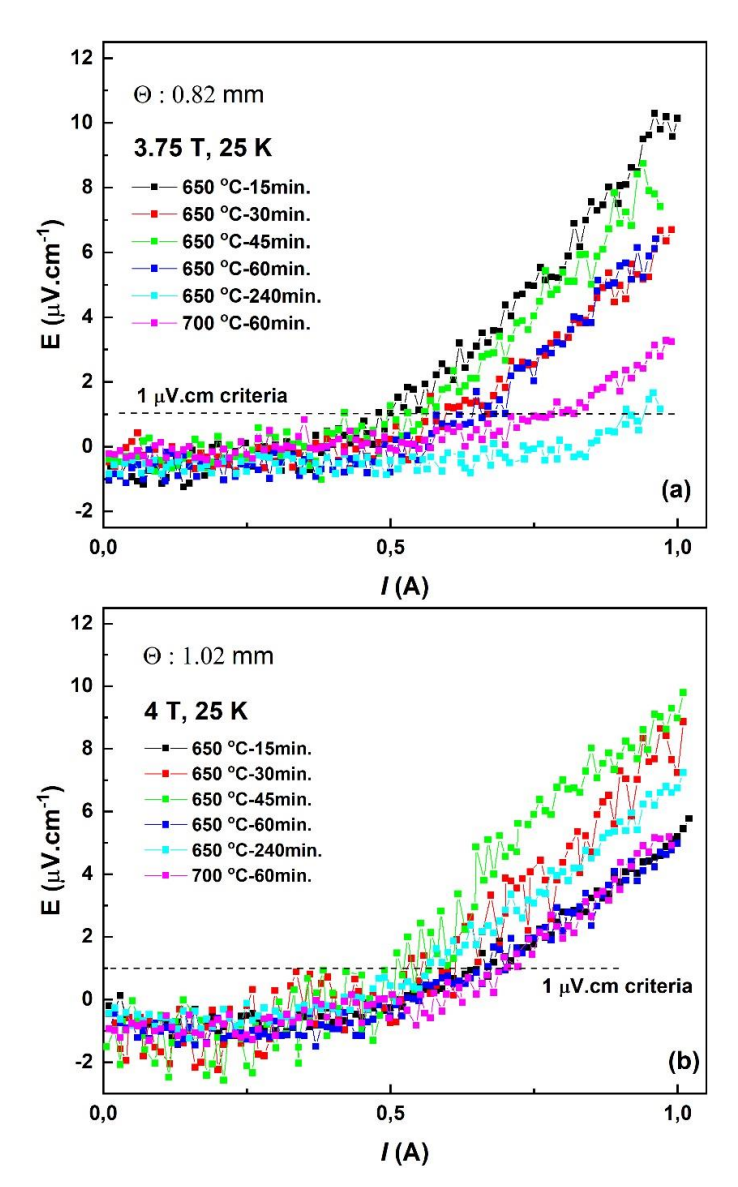


Figure 5. Electric field vs. current curves of multifilament wires with diameters of (a) 0.82 mm and (b) 1.02 mm. The wires were annealed at different temperature and time.

Images taken with an optical microscope from a single filament of multifilament wires with outer diameters of 0.82 mm and 1.02 mm subjected to different heat treatments are given in Figures 6 and 7, respectively. When the images are examined, the orange core regions in the wires show that MgB2 phase is successfully formed. It is seen that the use of large Mg particles results in the formation of a locally dense MgB2 structure, but also causes some unreacted boron regions to remain, appearing as black regions in the core structure. The size and distribution of unreacted boron regions are similar in the filaments of wires annealed under different heat treatment conditions. This reveals that short-term low-temperature (650 °C - 15 min) annealing is sufficient for MgB2 phase formation.

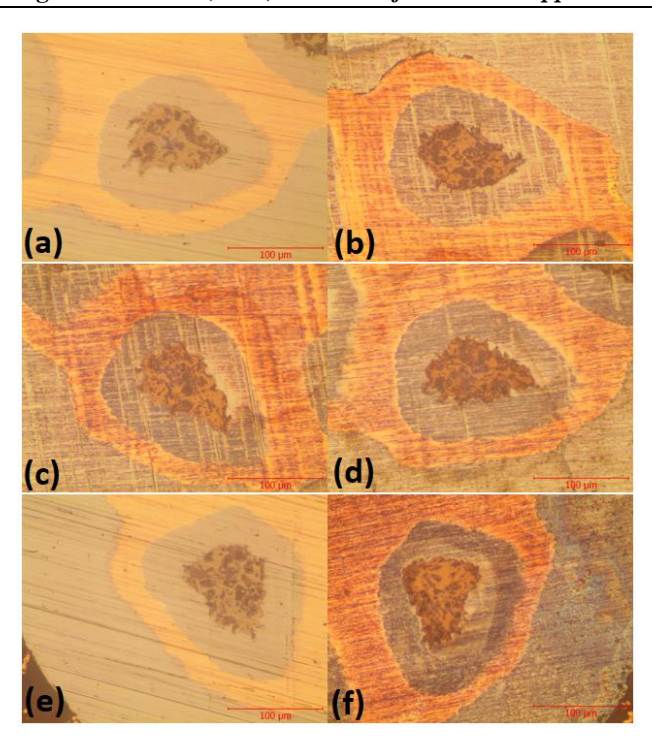


Figure 6. Single filament images taken with an optical microscope at 20x magnification from the cross-section of multifilament wires with a diameter of 0.82 mm. The multifilament wires are heat treated at different conditions, (a) 650 °C -15 min., (b) 650 °C -30 min, (c) 650 °C - 45 min., (d) 650 °C - 60 min., (e) 650 °C - 240 min., and (f) 700 °C - 60 min.

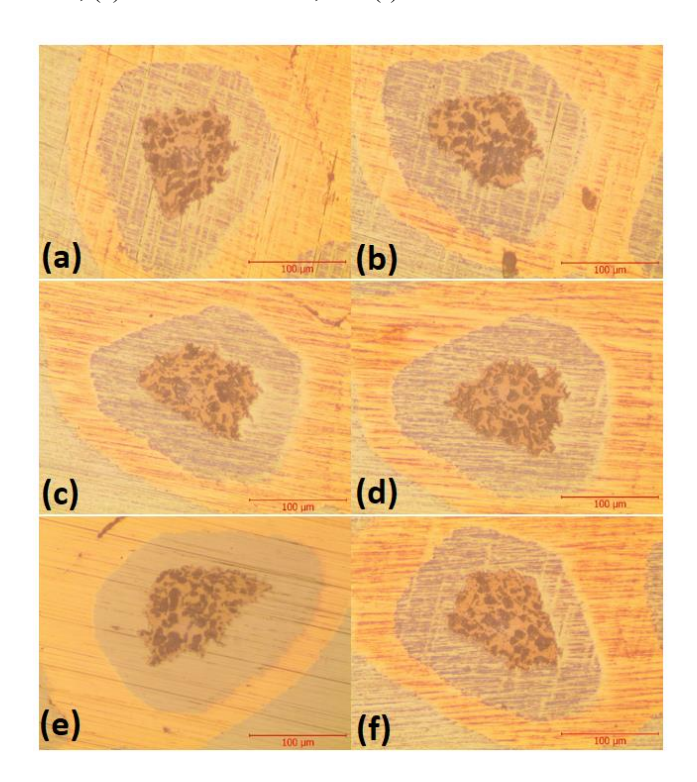


Figure 7. Single filament images taken with an optical microscope at 20x magnification from the cross-section of multifilament wires with a diameter of 1.02 mm. The multifilament wires are heat treated at different conditions, (a) 650 °C -15 min., (b) 650 °C -30 min, (c) 650 °C - 45 min., (d) 650 °C - 60 min., (e) 650 °C - 240 min., and (f) 700 °C - 60 min.

Figure 8 shows the Nb filaments obtained after etching the Fe and Cu sheath parts of the unreacted multifilament wire. An effective acidic solution was used in the etching process that selectively dissolved iron and copper without damaging the Nb

filaments (Chmielewski et al., 1997; Heini et al., 2017). The etching process was applied to wires with diameters of 1.50 mm, 1.02 mm, and 0.82 mm. Each wire was 6 cm in-length and the wire ends were securely sealed to avoid any reaction

between the MgB₂ core and acidic solution. After dissolving Fe and Cu layers, Nb filaments were successfully extracted as shown in Figure 8. Structural examination of these filaments was carried out using an optical microscope, and the images of Nb filaments are given in Figure 9. It is revealed that the sausage effect initiates at a diameter of 1.50 mm, as shown in the up row of Figure 9. A continuous cold drawing process from 1.50 mm to 0.82 mm diameter gradually increases the sausage effect and results in significant tear-ups on the surface of the Nb sheath, as shown in Figure 9. Some filaments exhibit notable deformations, such as cracks, sausage structures, and

tears (see Figure 10) but the many filaments for each diameter remain unaffected. These deformations arise due to non-uniformity in powder density within the wire (Shan et al., 2012). Furthermore, the agglomeration of B powder with large Mg particles can create non-uniform powder regions along the wire, making such deformations worse. In multifilament wires, filament deformations cannot be precisely detected from the outside; existing deformations in the filaments affect the flow of current throughout the entire wire and lead to adverse thermal instabilities which cause quench effects (Goldacker et al., 2004b).

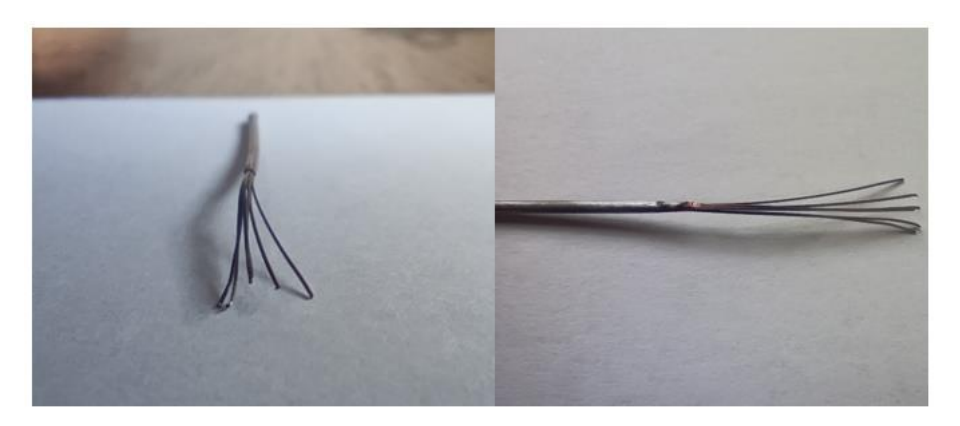


Figure 8. Nb/MgB₂ filaments of unreacted multifilament wire after etching process.

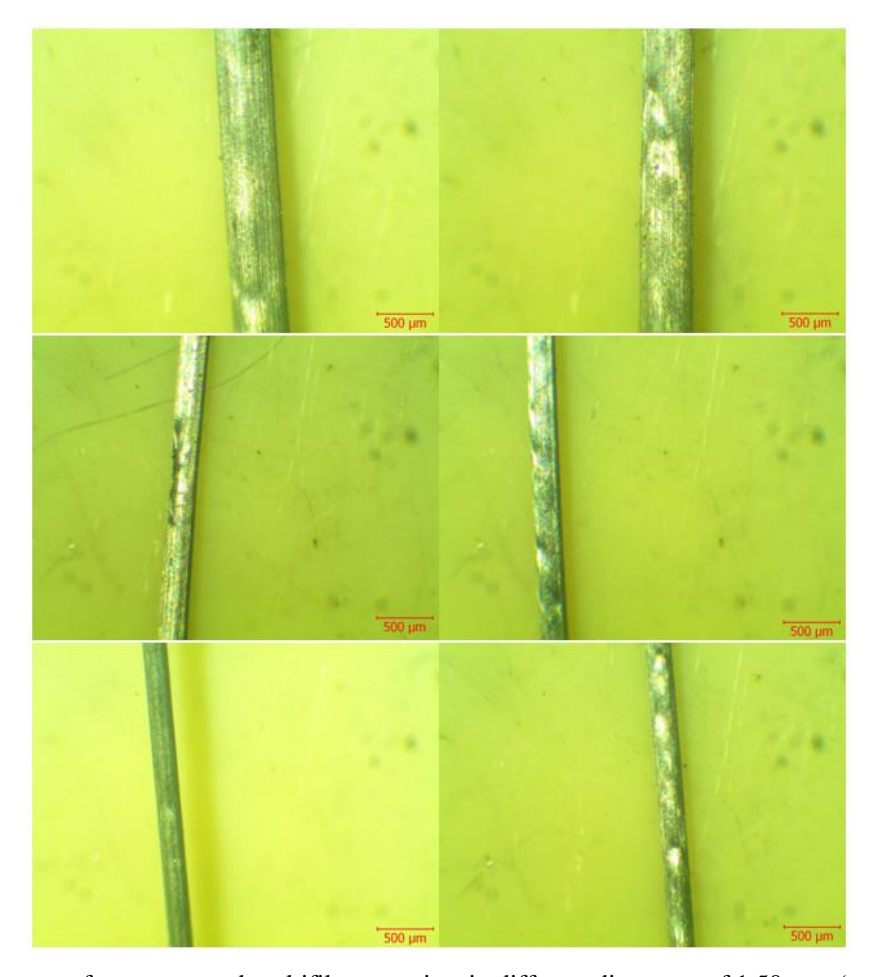


Figure 9. Nb mono filaments cut from unreacted multifilament wires in different diameters of 1.50 mm (top), 1.02 mm (middle), 0.82 mm (bottom).

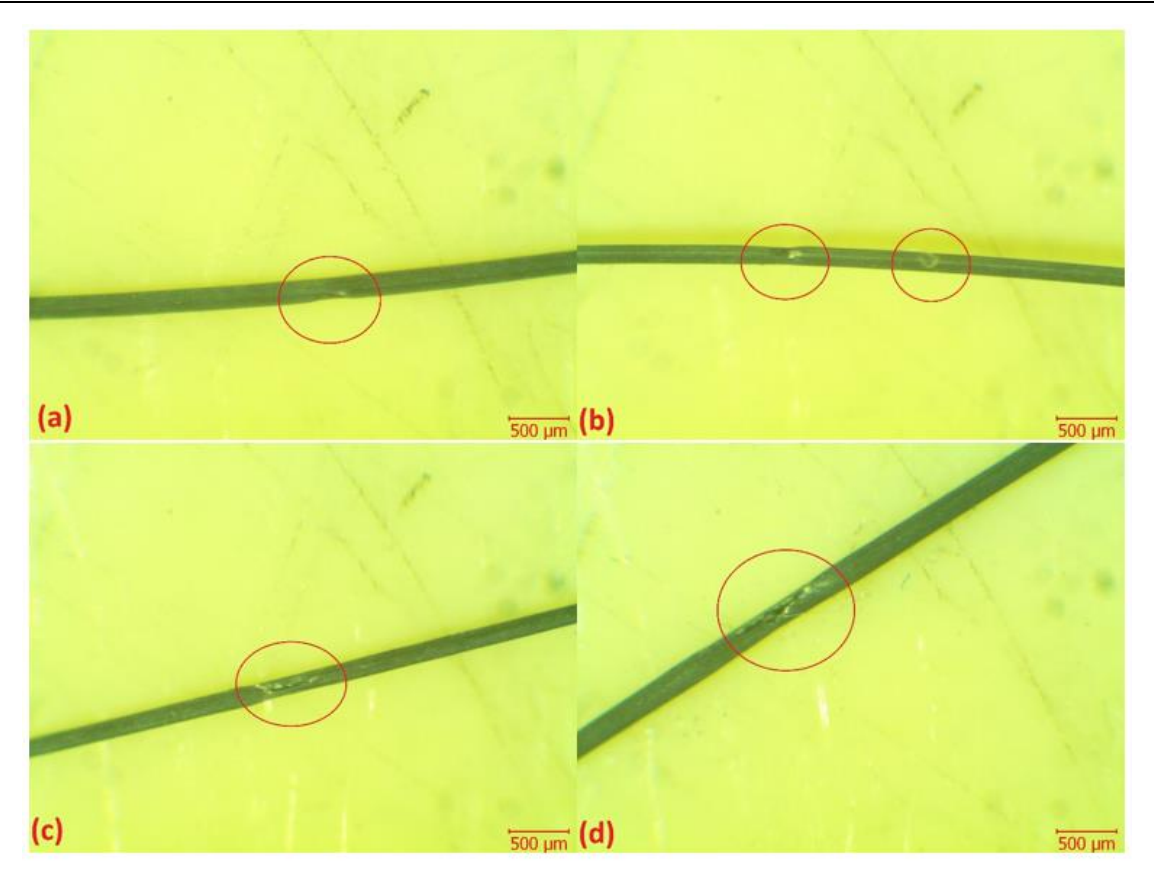


Figure 100. Deformities on Nb filaments. The wire pieces were prepared using (a) - (b) 200-325 mesh Mg powder. (c) - (d) 100-200 mesh Mg powder.

4. Conclusion

In this study, we examined possible structural problems on the inner surface of multifilament Fe/Cu/Nb/MgB2 wire produced by cold forming methods. It is observed that defects such as tearing and sausaging do not occur all along the wire, but they may occur at several arbitrary locations on some filaments. The production-related deformations worsen the transport properties of the wire as the wire diameter decreases. Our results suggest that the sausaging at large diameters may be a significant contributor to the tearing of the sheath material at small wire diameters. It is revealed that the superconducting core structures of the wires subjected to different thermal treatments are similar, so, a short-term low-temperature (650 °C - 15 min) annealing is sufficient for MgB₂ phase formation. Defects occurring in Nb/MgB2 filaments cannot be determined from the external structure of multifilament wires, but they negatively affect the transport properties of the wire. The use of finer Mg powder for initial Mg+2B mixture will benefit against filament deterioration (Fig. 10). The etching has emerged as an effective technique to study the structural properties of internal Nb filaments without damaging them. This is also important for joining MgB2 multifilament wires. As a result, we showed that Fe/Cu/Nb/MgB2 wires up to 0.82 mm in diameter can be produced without any major structural problems by cold forming method without applying strain-relief heat treatment.

Acknowledgment

This study was supported under titled "Bitter Type New Generation MgB2 Superconducting Solenoid Coil Construction and Characterisation" by the TUBİTAK, Grant No: 219M270.

Conflict of Interest

The authors declare that they have no conflict of interest.

References

Chmielewski, A. G., Urbtiski, T. S., & Migdal, W. (1997). Separation technologies for metals recovery from industrial wastes. *Hydrometallurgy*, 45(3), 333-344. https://doi.org/10.1016/S0304-386X(96)00090-4

Feng, Y., Yan, G., Zhao, Y., Liu, C. F., Fu, B.Q., Zhou, L., Cao, L. Z., Ruan, K. Q., Li, X. G., Shi, L., & Zhang Y. H. (2003). Superconducting properties of MgB₂ wires and tapes with different metal sheaths. *Physica C: Superconductivity*, 386, 598-602. https://doi.org/10.1016/S0921-4534(02)02169-X

Goldacker, E., Schlachter, S. I., Obst B., & Eisterer, M. (2004a). *In situ* MgB₂ round wires with improved properties. *Superconductor Science and Technology*, 17, S490-S495. https://doi.org/10.1088/0953-2048/17/9/006

- Goldacker, W., Sonja, I., Bing Liu, S., Obst, B., & Klimenko, E. (2004b). Considerations on critical currents and stability of MgB₂ wires made by different preparation routes. *Physica C: Superconductivity*, 401(1-4), 80-86. https://doi.org/10.1016/j.physc.2003.09.014
- Heini, E., Sipi, S., Tero, J., Tuomas, S., Benjamin, P. W., Jari, A., & Mari, L. (2017). The effect of the redox potential of aqua regia and temperature on the Au, Cu, and Fe dissolution from WPCBs. *Recycling*, 2(3), 14. https://doi.org/10.3390/recycling2030014
- Jiawen, X., Xiaoze, P., Jie, S., Hideki, T., Yota, I., Min, Z., & Weijia, Y. (2019). Experimental test and analysis of AC losses in multifilamentary MgB₂ wire. *IEEE Transactions on Applied Superconductivity*, 29(5), 8201205. https://doi.org/10.1109/TASC.2019.2903924
- Koblischka, M. R., Alexander, W., Miryala, M., Inoue, K., Thomas, H., Bruno, D., Kevin, B., Masato, M., & Uwe, H. (2014). Development of MgB₂-based bulk supermagnets. *IEEE Transactions on Magnetics*, 50(11), 9000504. https://doi.org/10.1109/TMAG.2014.2323995
- Masayoshi, I., & Yuichi, O. (2023). Filament structure analysis of multifilament MgB₂ wires by using X-ray CT. *IEEE Transactions on Applied Superconductivity*, 33(5), 6200104. https://doi.org/10.1109/TASC.2023.3248540
- Nakane, T., Fujii, H., Matsumoto, A., Kitaguchi, H., & Kumakura, H. (2005). The improvement of in-situ powder in tube MgB₂ tapes by mixing MgB₂ to the starting powder of MgH₂ and B. *Physica C: Superconductivity and its Applications*, 426-431(Part 2), 1238-1243. https://doi.org/10.1016/j.physc.2005.02.147
- Patel, D., Al Hossain, M. S., Motaman, A., Barua, S., Shahabuddin, M., & Kim, J. H. (2014). Rational design of MgB₂

- conductors toward practical applications. *Cryogenics*, *63*, 160-165. https://doi.org/10.1016/j.cryogenics.2014.04.016
- Shan, D., Yan, G., Zhou, L., Li, J. S., Li, C. S., Wang, Q. Y., Xiong, X. M., & Jiao, G. F. (2012). Multifilamentary MgB₂ wires fracture behavior during the drawing process. *Physica C: Superconductivity*, 483, 17-20. https://doi.org/10.1016/j.physc.2012.06.007
- Suo, H. -L., Ma, L., Jiang, J. -M., Li, Y. -M., Zhang, Z. -L., Liu, M., Zhao, Y., He, D. -Y., & Zhou, M. -L. (2007). High Critical Current Densities in SiC Doped *In-Situ* MgB₂ wires prepared by continuous tube forming and filling technique. *IEEE Transactions on Applied Superconductivity*, 17(2), 2822-2825. https://doi.org/10.1109/tasc.2007.897457
- Tomsic, M., Rindflesich, M., Yue, J., McFadden, K., Phillip, J., Sumption, M. D., Bhatia, M., Bohnenstiehl, S., & Collings, E. W. (2007). Overview of MgB₂ superconductor applications. *International Journal of Applied Ceramic Technology*, 4(3), 250-259. https://doi.org/10.1088/0953-2048/18/5/026
- Vinod, K., Abhilash Kumar, R. G., & Syamaprasad, U. (2007).

 Prospects for MgB₂ superconductors for magnet application. *Superconductor Science and Technology*, 20(1), R1-R13. https://doi.org/10.1088/0953-2048/20/1/R01
- Xi, X. X. (2009). MgB₂ thin films. *Superconductor Science and Technology*, 22(4), 043001. https://doi.org/10.1088/0953-2048/22/4/043001
- Yao, W., Bascuñán, J., Hahn, S., & Iwasa, Y. (2010). MgB₂ coils for MRI applications. *IEEE Transactions on Applied Superconductivity*, 20(3), 756-759. https://doi.org/10.1109%2FTASC.2010.2044035